

Structural and magnetic properties of Bi doped in the A site of $(\text{Pr}_{1-x}\text{Bi}_x)_{0.6}\text{Sr}_{0.4}\text{MnO}_3$ ($0 \leq x \leq 0.4$) perovskite manganites

Imed Kammoun · Wissem Cheikhrouhou-Koubaa ·
Wahiba Boujelben · Abdelwaheb Cheikhrouhou

Received: 2 March 2007 / Accepted: 26 September 2007 / Published online: 9 November 2007
© Springer Science+Business Media, LLC 2007

Abstract We studied the effect of Bi doping in the A-site on the structural, magnetic, and magneto-caloric properties of the $(\text{Pr}_{1-x}\text{Bi}_x)_{0.6}\text{Sr}_{0.4}\text{MnO}_3$ ($0 \leq x \leq 0.4$) perovskite manganese oxides. In this study, the average ionic radius $\langle r_A \rangle$ of the A cation site was systematically varied while keeping fixed the carrier concentration ($\text{Mn}^{3+}/\text{Mn}^{4+}$ ratio). All our samples have been elaborated by the conventional solid state reaction at high temperature. X-ray powder diffraction at room temperature showed that all our synthesized samples are single phase and crystallize in the orthorhombic system with Pbnm space group. The unit cell volume decreases linearly with increasing Bi content. Magnetization measurements versus temperature in a magnetic applied field of 50 mT show that all our samples exhibit a paramagnetic to ferromagnetic transition when temperature decreases. The Curie temperature T_C decreases from 310 K for $x = 0$ to 252 K for $x = 0.4$. The critical exponent γ defined by $M_{\text{sp}}(T) = M_{\text{sp}}(0)(1 - T/T_C)^\gamma$ and deduced from M(H) curves is found to be 0.315 for $\text{Pr}_{0.54}\text{Bi}_{0.06}\text{Sr}_{0.4}\text{MnO}_3$ sample. Furthermore, a large magnetocaloric effect near T_C has been detected with a maximum of magneto-entropy change, of $1.11 \text{ Jkg}^{-1} \text{ K}^{-1}$ and $4.78 \text{ Jkg}^{-1} \text{ K}^{-1}$ at 1 T and 7 T, respectively, for $\text{Pr}_{0.54}\text{Bi}_{0.06}\text{Sr}_{0.4}\text{MnO}_3$ sample.

Introduction

The discovery of colossal magnetoresistance effects in perovskite manganese oxides with general formula $\text{Ln}_{1-x}\text{A}_x\text{MnO}_3$ (Ln is a trivalent rare earth element and A is a divalent alkaline-earth or a monovalent alkali metal) has attracted considerable attention during the last decade. These materials exhibit many significant properties like metal–insulator transition, ferromagnetic–paramagnetic phase change, charge and orbital ordering, etc. depending on the charge density, temperature and atomic structure [1–6]. The average ionic radius $\langle r_A \rangle$ of the A-cation site [7], the mismatch effect [8], the vacancy in the A and B sites, the polaron effect due to the strong electron–phonon coupling arising from Jahn–Teller distortions [9] and the oxygen stoichiometry [10–12] play also a crucial role.

The electrical and magnetic properties had been understood within a framework of the double exchange model [13–14]. The motion of the e_g electron can be strongly influenced by the average ionic radius of the A site which exhibits a closed relationship between the bending of the Mn–O–Mn bond angle and the narrowing of the electronic band width [15].

The parent compound $\text{Pr}_{0.6}\text{Sr}_{0.4}\text{MnO}_3$ exhibits a paramagnetic–semiconductor to ferromagnetic–metallic transition with decreasing temperature [16–17]. The Curie temperature T_C is found to be 310 K. Previous work on the effect of the Bi-doping in the B-site on the physical properties of $\text{Pr}_{0.6}\text{Sr}_{0.4}\text{Mn}_{1-x}\text{Bi}_x\text{O}_3$ ($0 \leq x \leq 0.2$) powder samples [18] showed that the Bi doping leads to a weakening of the ferromagnetic ordering at low temperature and the Curie temperature T_C decreases from 310 K for $x = 0$ to 225 K for $x = 0.2$.

In this article, we studied the structural, magnetic, and magneto-caloric properties of $(\text{Pr}_{1-x}\text{Bi}_x)_{0.6}\text{Sr}_{0.4}\text{MnO}_3$

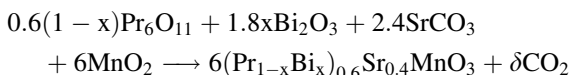
I. Kammoun · W. Cheikhrouhou-Koubaa · W. Boujelben ·
A. Cheikhrouhou (✉)
Laboratoire de Physique des Matériaux, Faculté des Sciences
de Sfax, B.P. 802, 3018 Sfax, Tunisia
e-mail: abdcheikhrouhou@yahoo.fr

A. Cheikhrouhou
Laboratoire de Magnétisme Louis NEEL, B.P. 166, 38042
Grenoble Cedex 9, France

powder samples with $0 \leq x \leq 0.4$. In these systems the Mn^{4+} content remains constant equal to 40%, however the average ionic radius of the A cation decreases with increasing Bi doping from 1.231Å for $x = 0$ to 1.229Å for $x = 0.4$.

Experimental

Polycrystalline $(Pr_{1-x}Bi_x)_{0.6}Sr_{0.4}MnO_3$ ($0 \leq x \leq 0.4$) compounds were prepared by the conventional solid-state reaction method in air at high temperature by mixing Pr_6O_{11} , Bi_2O_3 , $SrCO_3$, and MnO_2 up to 99.9% purity in the desired proportion according the following reaction:



The starting materials, Pr_6O_{11} , Bi_2O_3 , $SrCO_3$, and MnO_2 , weighted in the stoichiometric proportions, were intimately mixed in an agate mortar and heated in air at 1,000 K for 72 h. After grinding, the powders were pressed into pellets forms (of about 1 mm thickness and 13 mm diameter) under 4 tons/cm² and sintered at 1,400°C in air for 3 days with intermediate regrinding and repelling. Finally, the pellets were rapidly quenched to room temperature in air. This step was carried out in order to conserve the structure at the annealed temperature.

Phase purity, homogeneity, and cell dimensions were determined by X-ray powder diffraction at room temperature (diffractometer using Cu-Kα radiation, $\lambda = 1.5418\text{Å}$) and $20^\circ \leq 2\theta \leq 120^\circ$ with steps of 0.017° . The structure refinement was carried out using the Rietveld technique [19].

Magnetization measurements versus temperature and versus magnetic applied field up to 7 T were recorded using an extraction magnetometer in the temperature range 20–300 K.

Results and discussion

In order to check the Mn^{4+} content in our samples, we performed chemical analysis on our samples. We list in Table 1 the chemical analysis results. The experimental

Table 1 Chemical analysis results for $(Pr_{1-x}Bi_x)_{0.6}Sr_{0.4}MnO_3$ samples

X	Mn ⁴⁺ (Th)	Mn ⁴⁺ (Exp)	Relative error(%)
0.00	0.40	40.88	+2.2
0.10	0.40	38.88	-2.8
0.20	0.40	41.38	+3.4
0.30	0.40	39.19	-2
0.40	0.40	41.21	+3

results showed that the Mn^{4+} content remains constant for all the samples indicating that the bismuth in our samples is effectively in the trivalent state.

Structural analysis at room temperature showed that all our synthesized samples $(Pr_{1-x}Bi_x)_{0.6}Sr_{0.4}MnO_3$ ($0 \leq x \leq 0.4$) are single-phase and crystallize in the orthorhombic perovskite structure with Pbnm space group. By Bi doping in the A cation-site no apparent structural changes can be identified. Structure refinements using the Rietveld method have been achieved with the Fullprof program [20]. Figure 1 shows the X-ray diffraction patterns (measured, calculated and Bragg reflection positions) at room temperature for $(Pr_{1-x}Bi_x)_{0.6}Sr_{0.4}MnO_3$ samples ($x = 0$ and 0.4). A good fit between the observed and the calculated profiles was obtained. The difference observed between the intensities of the measured and calculated diffraction lines can be attributed to the existence of preferential orientation of the crystallites in the samples. Details of the refined results are summarized in Table 2. With increasing Bi

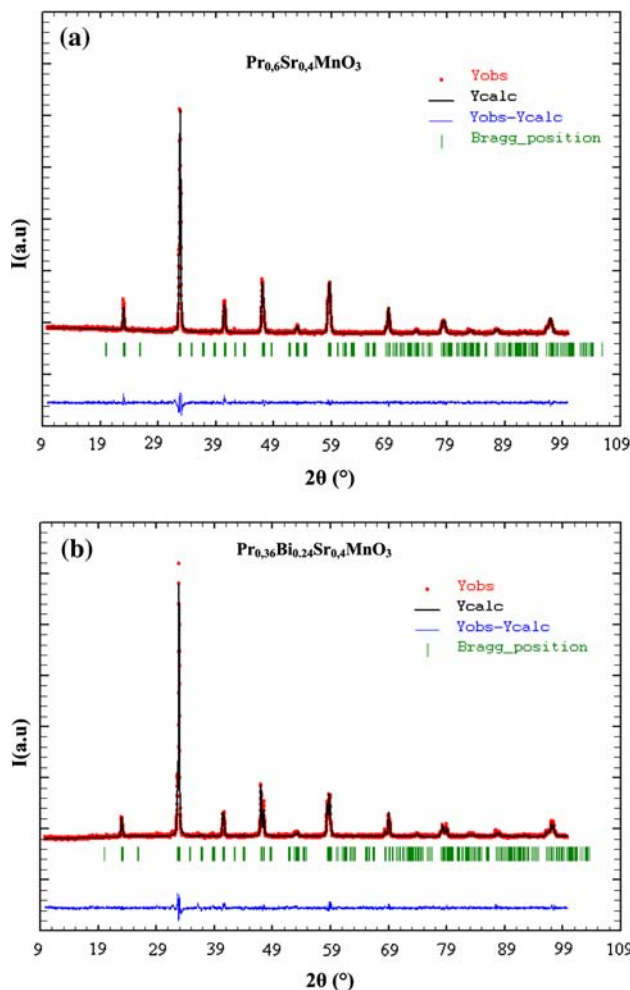


Fig. 1 X-ray powder diffraction pattern and refinement at room temperature for (a) $Pr_{0.6}Sr_{0.4}MnO_3$ and (b) $Pr_{0.36}Bi_{0.24}Sr_{0.4}MnO_3$ samples

Table 2 Crystallographic data for $(\text{Pr}_{1-x}\text{Bi}_x)_{0.6}\text{Sr}_{0.4}\text{MnO}_3$ samples

Samples	$x = 0.0$	$x = 0.1$	$x = 0.2$	$x = 0.3$	$x = 0.4$
a (Å)	5.4500(0)	5.4424(9)	5.4410(9)	5.4382(3)	5.4350(3)
b (Å)	5.4803(6)	5.4846(3)	5.4860(1)	5.4802(8)	5.4807(6)
c (Å)	7.6926(4)	7.6726(9)	7.6589(1)	7.6496(2)	7.6403(8)
Volume* (Å ³)	229.76	229.03	228.61	227.98	227.59
Pr/Sr/ Bi					
x	0.49623	0.50538	0.50330	0.51140	0.50780
y	0.00117	0.00340	0.00093	-0.00160	0.00012
z	0.25000	0.25000	0.25000	0.25000	0.25000
B _{iso} (Å ²)	0.99294	1.19548	0.91267	0.80865	0.20072
Mn					
x	0	0	0	0	0
y	0	0	0	0	0
z	0	0	0	0	0
B _{iso} (Å ²)	0.86617	0.89472	0.66561	0.33507	0.76105
O (1)					
x	0.49264	0.49495	0.50756	0.48971	0.50854
y	0.43285	0.54509	0.54006	0.52812	0.47411
z	0.25000	0.25000	0.25000	0.25000	0.25000
B _{iso} (Å ²)	0.16546	1.16406	0.41960	0.74641	0.44393
O (2)					
x	0.27830	0.24876	0.23275	0.22830	0.22028
y	0.22727	0.22369	0.21568	0.21443	0.20943
z	0.03788	0.02712	0.03098	0.00757	0.02561
B _{iso} (Å ²)	0.16546	1.16406	0.41960	0.74641	0.44393
Residues of refinement					
R _p (%)	2.45	1.90	2.07	2.23	2.22
R _{wp} (%)	3.64	2.50	2.72	3.09	3.12
R _F (%)	2.51	2.49	2.50	2.38	2.42
χ ²	1.99	1.01	1.19	1.69	1.65

content, a and c lattice parameters decrease while b lattice parameter remains almost constant. We plot in Fig. 2 the evolution of the cell parameters as a function of Bi content. Bismuth doping leads to a slight decrease of the unit cell volume, it decreases linearly from 229.76 Å³ for $x = 0$ to 227.59 Å³ for $x = 0.4$ (Fig. 2). This behavior can be explained by the decrease of the average ionic radius of the A cation site, in fact the ionic radius of Bi³⁺ (1.170 Å) is smaller the Pr³⁺ (1.179 Å) one. The average ionic radius of the A-cation site, given by $\langle r_A \rangle = 0.6(1-x)r(\text{Pr}^{3+}) + 0.6x r(\text{Bi}^{3+}) + 0.4 r(\text{Sr}^{2+})$, decreases from 1.231 Å for $x = 0$ to 1.229 Å for $x = 0.4$.

The decrease of the cell parameters is linked to the decrease of the Mn–O distances (denoted by $d_{\text{B-O1}}$ and $d_{\text{B-O2}}$) and the (Mn)–(Pr/Bi) distances (denoted by $d_{\text{B-A}}$). The distances $d_{\text{B-O1}}$, $d_{\text{B-O2}}$, $d_{\text{B-A}}$, and the angles B–O–B, O–B–O refined for the different samples are listed in Table 3. The influence of the ionic radius of the A site can be

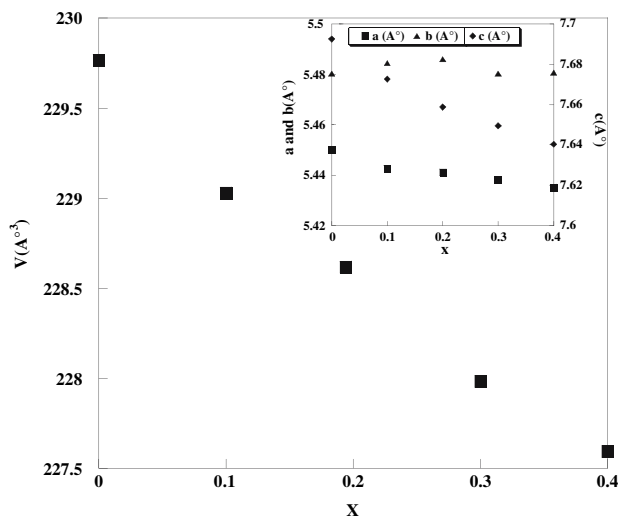


Fig. 2 Unit-cell volume V evolution as a function of x for $(\text{Pr}_{1-x}\text{Bi}_x)_{0.6}\text{Sr}_{0.4}\text{MnO}_3$ samples ($0 \leq x \leq 0.4$). Inset the evolution of the lattice parameters a , b , and c versus x

Table 3 Values of average distances and angles in $(Pr_{1-x}Bi_x)_{0.6}Sr_{0.4}MnO_3$ samples

x	d_{Mn-O1} (Å)	d_{Mn-O2} (Å)	d_{Mn-A} (Å)	Mn-O1-Mn (°)	Mn-O2-Mn (°)	$\langle Mn-O-Mn \rangle$ (°)
0.00	1.958	1.964	3.348	165.43	126.69	139.60
0.10	1.934	1.945	3.346	170.13	123.86	139.28
0.20	1.928	1.938	3.345	171.11	121.63	138.12
0.30	1.919	1.931	3.342	173.46	120.36	138.06
0.40	1.914	1.927	3.340	174.04	119.99	138.00

explained by its ability to modify the Mn-O, Mn-A distances and the Mn-O-Mn angle and consequently the distortion of the ideal perovskite structure in which the Mn-O-Mn angle is equal to 180° .

Magnetic properties

Magnetization measurements as a function of temperature in the range 20–300 K in a magnetic applied field of 50 mT showed that all our samples exhibit a sharp transition from paramagnetic to ferromagnetic state with increasing temperature. This sharp transition confirms well the good quality of our samples. We plot in Fig. 3 the temperature dependence of the magnetization for all our synthesized samples $(Pr_{1-x}Bi_x)_{0.6}Sr_{0.4}MnO_3$ ($0 \leq x \leq 0.4$). The magnetization in the parent compound shows a small decrease below 100K which has been attributed from neutron diffraction studies to the coexistence, at low temperature, of two phases: an orthorhombic phase with Pnma space group (27%) and a monoclinic one with I2/a space group (73%) [16]. In the low doped samples ($x \leq 0.1$) the magnetization

decrease occurs at higher temperatures than disappears for $x > 0.1$.

Using the inflection point of the $M(T)$ curve to determine the Curie temperature T_C , Bi doping leads to a decrease of the T_C . The Curie temperature is found to decrease from 310 K for $x = 0$ to 252 K for $x = 0.4$. Previous work [18] showed that the Bi doping in the Mn site in the $Pr_{0.6}Sr_{0.4}Mn_{1-x}Bi_xO_3$ ($0 \leq x \leq 0.2$) leads also to a decrease of the Curie temperature T_C from 310 K for $x = 0$ to 225 K for $x = 0.2$. In Fig. 4, we plot the evolution of the T_C versus Bi content in both series $(Pr_{1-x}Bi_x)_{0.6}Sr_{0.4}MnO_3$ and $Pr_{0.6}Sr_{0.4}Mn_{1-x}Bi_xO_3$ powder samples.

As the Mn^{4+} content remains constant in all our Bi doping samples $(Pr_{1-x}Bi_x)_{0.6}Sr_{0.4}MnO_3$, the decrease of T_C with increasing Bi content may be explained by the decrease of the ionic average radius $\langle r_A \rangle$ of the A cation site. In fact $\langle r_A \rangle$ decreases from 1.231Å for $x = 0$ to 1.229Å for $x = 0.4$. Previous work on the effect of the Bi doping on the physical properties of $(Pr_{1-x}Bi_x)_{0.7}Sr_{0.3}MnO_3$ showed also a decrease of T_C with increasing Bi content and such behavior has been explained in terms of average ionic radius $\langle r_A \rangle$ of the A cation site [21]. This behavior may be also explained in terms of $\langle Mn-O-Mn \rangle$ bond angle; in fact a

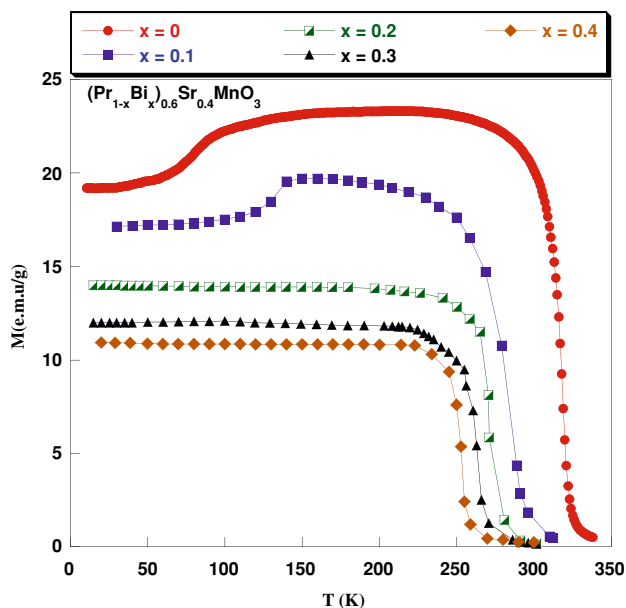


Fig. 3 Temperature dependence of the magnetization at $\mu_0H = 50$ mT for $(Pr_{1-x}Bi_x)_{0.6}Sr_{0.4}MnO_3$ ($0.0 \leq x \leq 0.4$)

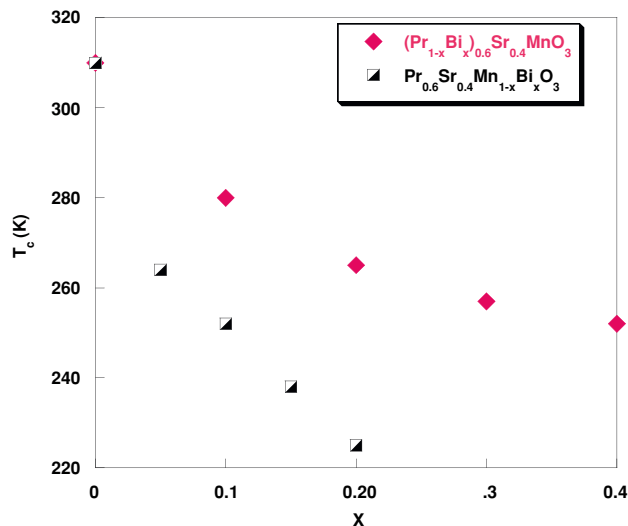


Fig. 4 Curie temperature dependence as a function of x for both series $(Pr_{1-x}Bi_x)_{0.6}Sr_{0.4}MnO_3$ and $Pr_{0.6}Sr_{0.4}Mn_{1-x}Bi_xO_3$ samples ($0 \leq x \leq 0.4$)

decrease in this average angle leads to a shift of T_C to lower values [22].

In order to confirm the ferromagnetic behavior at low temperatures of our samples, we performed magnetization measurements versus magnetic applied field up to 8 T at several temperatures. We plot in Fig. 5 the $M(H)$ curves for $\text{Pr}_{0.54}\text{Bi}_{0.06}\text{Sr}_{0.4}\text{MnO}_3$ ($x = 0.1$). The magnetization rises sharply for low magnetic applied field and then saturates for $\mu_0 H$ higher than 1 T. The saturation magnetization at 20 K, deduced from the $M(H)$ curve, is found to be $2.94 \mu_B/\text{Mn}$, whereas the spontaneous magnetization calculated for full spin alignment is found to be $3.60 \mu_B/\text{Mn}$. Using Anderson model [23], the angle θ_{ij} between the Mn^{3+} - Mn^{4+} moments deduced from $t_{ij} = b \cos \frac{\theta_{ij}}{2}$ is found to be equal to 61° . The discrepancy may be due to a spin canted state between the Mn^{3+} and Mn^{4+} ions. In the parent compound $\text{Pr}_{0.6}\text{Sr}_{0.4}\text{MnO}_3$ the experimental and theoretical values of the spontaneous magnetization are, respectively, 3.58 and $3.60 \mu_B/\text{Mn}$ [16].

In order to determine the Curie temperature with precision, we plot in Fig. 6 the Arrott curves (M^2 versus H/M) for the $\text{Pr}_{0.54}\text{Bi}_{0.06}\text{Sr}_{0.4}\text{MnO}_3$ compound. T_C deduced from these curves is found to be 270 K which is almost the same than that determined from $M(T)$ curve.

Figure 7 shows the evolution, as a function of temperature, of the spontaneous magnetization M_{sp} deduced from the $M(H)$ curves and the inverse of the susceptibility ($1/\chi$) for $\text{Pr}_{0.54}\text{Bi}_{0.06}\text{Sr}_{0.4}\text{MnO}_3$ sample. The critical exponent γ given by $M_{sp}(T) = M_{sp}(0)(1 - T/T_C)^\gamma$ is found to be

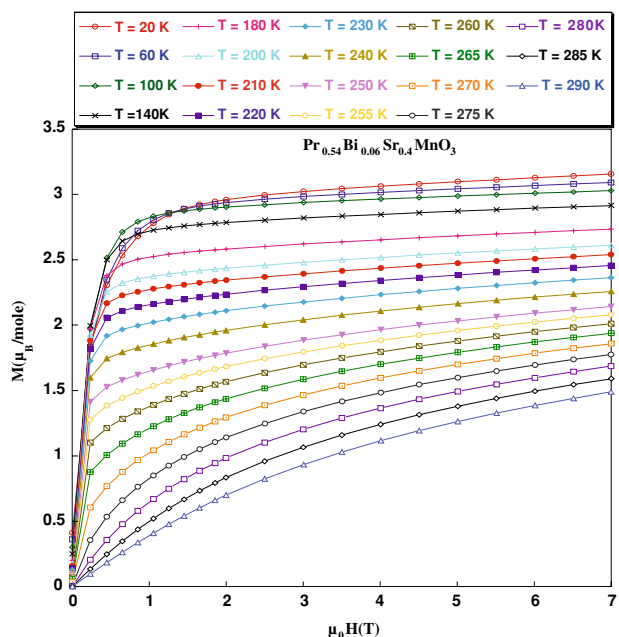


Fig. 5 Magnetization versus magnetic applied field up to 7 T at several temperatures in $\text{Pr}_{0.54}\text{Bi}_{0.06}\text{Sr}_{0.4}\text{MnO}_3$ sample

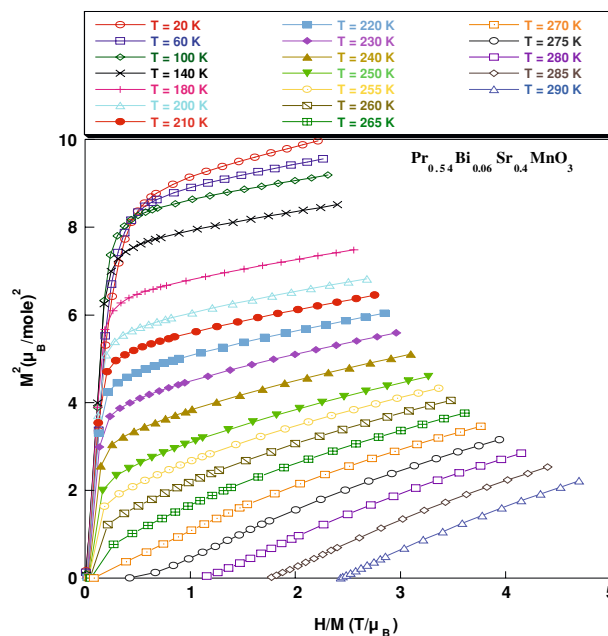


Fig. 6 Arrott curves for $\text{Pr}_{0.54}\text{Bi}_{0.06}\text{Sr}_{0.4}\text{MnO}_3$ sample

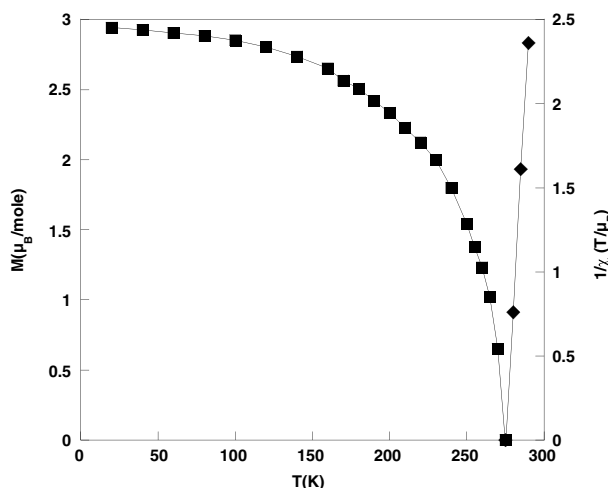


Fig. 7 Spontaneous magnetization and inverse susceptibility versus temperature for the $\text{Pr}_{0.54}\text{Bi}_{0.06}\text{Sr}_{0.4}\text{MnO}_3$ sample

0.315 which confirms well the ferromagnetic behavior at low temperatures of our sample. In the parent compound $\text{Pr}_{0.6}\text{Sr}_{0.4}\text{MnO}_3$ the critical exponent γ is found to be 0.33.

Magnetocaloric effect

Based on magnetization measurements versus magnetic applied field at several temperatures, we have calculated the magnetic entropy change $|\Delta S_m|$ induced by the variation of the external magnetic field according to the classical thermodynamic theory:

$$\Delta S_m(T, H) = S_m(T, H) - S_m(T, 0) = \int_0^{H_{\max}} \left(\frac{\partial S}{\partial H} \right)_T dH \tag{1}$$

With Maxwell’s thermodynamic relationship: $\left(\frac{\partial S}{\partial B} \right)_T = \left(\frac{\partial M}{\partial T} \right)_B$, Eq. (1) can be written as:

$$\Delta S_m(T, H) = \int_0^{H_{\max}} \left(\frac{\partial M}{\partial T} \right)_H \mu_0 dH \tag{2}$$

When the magnetization is measured at small discrete field and temperature intervals, numerical approximation to the integral in Eq. (2) could be expressed as $|\Delta S_m| = \sum \frac{M_i - M_{i+1}}{T_{i+1} - T_i} \mu_0 \Delta H_i$ where M_i and M_{i+1} are the experimental values of magnetization at temperatures T_i and T_{i+1} , respectively, under a magnetic applied field H_i . Figure 8 illustrates the entropy change $|\Delta S_m|$ of polycrystalline perovskite $\text{Pr}_{0.54}\text{Bi}_{0.06}\text{Sr}_{0.4}\text{MnO}_3$ as a function of temperature under several magnetic applied field changes. As magnetic field change increased, the magnetic entropy change $|\Delta S_m|$ increases non linearly and reaches its maximum around 272 K. The maximum values of $|\Delta S_m|$ are $1.11 \text{ Jkg}^{-1}\text{K}^{-1}$ and $4.78 \text{ Jkg}^{-1}\text{K}^{-1}$ upon the magnetic field changes of 1 T and 7 T, respectively, for $\text{Pr}_{0.54}\text{Bi}_{0.06}\text{Sr}_{0.4}\text{MnO}_3$ sample ($x = 0.1$). These values are comparable to those obtained in $\text{La}_{0.7}\text{Sr}_{0.2}\text{Ag}_{0.1}\text{MnO}_3$ [24] ($|\Delta S_m| = 0.9 \text{ Jkg}^{-1}\text{K}^{-1}$ at 315 K under $H = 1 \text{ T}$) or $\text{La}_{0.95}\text{Ag}_{0.05}\text{MnO}_3$ [25] ($|\Delta S_m| = 1.1 \text{ Jkg}^{-1}\text{K}^{-1}$ at 214 K under $H = 1 \text{ T}$), but smaller than that reported by Gencer et al. [26] where they observed a large magnetocaloric effect in $\text{La}_{0.62}\text{Bi}_{0.05}\text{Ca}_{0.33}\text{MnO}_3$ which reaches $3.5 \text{ Jkg}^{-1}\text{K}^{-1}$ at 248 K under 1 T. The observed effect is larger than that obtained in the parent compound $\text{La}_{0.67}\text{Ca}_{0.33}\text{MnO}_3$. It should be noted that though the magnetocaloric effect was enhanced, the low value of the T_C makes it difficult to be used.

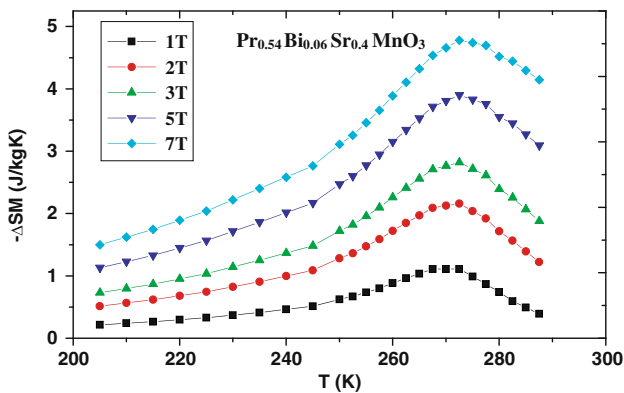


Fig. 8 Magnetocaloric effect evolution versus temperature for the $\text{Pr}_{0.54}\text{Bi}_{0.06}\text{Sr}_{0.4}\text{MnO}_3$ sample

Conclusion

We have elaborated and studied the physical properties of the $(\text{Pr}_{1-x}\text{Bi}_x)_{0.6}\text{Sr}_{0.4}\text{MnO}_3$ ($0 \leq x \leq 0.4$) perovskite manganese oxides. All our synthesized samples are single phase and crystallize in the orthorhombic symmetry with Pbnm space group. Bi doping leads to a decrease of the unit cell volume. All our samples exhibit a paramagnetic to ferromagnetic transition with decreasing temperature. The Curie temperature T_C is found to shift to lower values with increasing bismuth content. The spontaneous magnetization at 20 K deduced from the $M(H)$ curves for $\text{Pr}_{0.54}\text{Bi}_{0.06}\text{Sr}_{0.4}\text{MnO}_3$ sample is found to be $2.94 \mu_B/\text{Mn}$, which is smaller than the theoretical one found to be $3.6 \mu_B/\text{Mn}$ calculated for full spin alignment. The critical exponent γ defined by $M_{\text{sp}}(T) = M_{\text{sp}}(0)(1 - T/T_C)^\gamma$ is found to be 0.315 for $\text{Pr}_{0.54}\text{Bi}_{0.06}\text{Sr}_{0.4}\text{MnO}_3$ sample. In addition, our samples undergo a large magnetocaloric effect near room temperature.

Acknowledgement This work has been supported by the Tunisian Ministry of Higher Education, Scientific Research, and Technology.

References

1. Von Helmolt R, Wecker J, Holzapfel B, Schutz L, Samwer K (1993) Phys Rev Lett 71:2331
2. Maignan A, Simon Ch, Caignaert V, Raveau B (1996) J Magn Magn Mater 152:L5
3. Caignaert V, Suard E, Maignan A, Simon Ch, Raveau B (1996) J Magn Magn Mater 153:L260
4. Ju HL, Sohn H (1997) J Magn Magn Mater 167:200
5. Peles A, Kunkel HP, Zhou XZ, Williams G (1999) J Phys Condens Matter 11:8111
6. Huang YH, Yan CH, Wang ZM, Liao CS, Xu GX (2001) Solid State Comm 118:541
7. Damay F, Martin C, Martin A, Raveau B (1997) J Appl Phys 81:1372
8. Rodriguez-Martinez LM, Atfield JP (1996) Phys Rev B54: 15622
9. Millis AJ, Littlewood PB, Shraiman BI (1955) Phys Rev Lett 74:5144
10. Gonzalez-Calbet JM, Herrero E, Rangavittal N, Alonso JM, Martinez JL, Vallel-Kegi M (1999) J Solid State Chem 148:158
11. Abdelmoula N, Guidara K, Cheikhrouhou A, Dhahri E, Joubert JC (2000) J Solid State Chem 151:139
12. Troyanchuk IO, Trukanov SV, Szymezak H, Baerner K (2000) J Phys Condens Matter 12:L155
13. Zener C (1951) Phys Rev 82:403
14. Kubo K, Ohata N (1972) J Phys Soc Jpn 33:21
15. Hwang HY, Cheong SW, Radaelli PG, Marezio M, Batlogg B (1995) Phys Rev Lett 75:914
16. Boujelben W, Ellouze M, Cheikh-Rouhou A, Pierre J, Cai Q, Yelon WB, Shimizu K, Dubourdieu C (2002) J Alloys Comp 334:1
17. Boujelben W, Cheikh-Rouhou A, Ellouze M, Joubert JC (2000) Phys Stat Sol (a) 177:503
18. Kammoun I, Cheikhrouhou-Koubaa W, Boujelben W, Cheikhrouhou A, J Alloys Comp (in press)

19. Rietveld HM (1969) *J Appl Crystallogr* 2:65
20. Wiles DB, Young RA (1981) *J Appl Crystallogr* 14:149
21. Boujelben W, Ellouze M, Cheikh-Rouhou A, Fuess H (2002) *Phys Stat Sol (a)* 189:837
22. Yoshii K, Abe H, Ikeda N (2005) *J Solid State Chem* 176:3615
23. Anderson PW (1959) *Phys Rev* 115:2
24. Cheikh-Rouhou Koubaa W, Koubaa M, Cheikhrouhou A, *J Alloys Comp* (in press)
25. Tang T, Gu KM, Cao QQ, Wang DH, Zhang SY, Du YW (2000) *J Magn Magn Mater* 222:110
26. Gencer H, Atabay S, Adiguzel HI, Kolat VS (2005) *Physica B* 357:326